

Coupled-channels reactions for charged particles in harmonic traps

Hantao Zhang,^{1,*} Dong Bai^{2,†} and Zhongzhou Ren^{1,3,‡}

¹*School of Physics Science and Engineering, Tongji University, Shanghai 200092, China*

²*College of Mechanics and Engineering Science, Hohai University, Nanjing 211100, Jiangsu, China*

³*Key Laboratory of Advanced Micro-Structure Materials, Ministry of Education, Shanghai 200092, China*



(Received 9 April 2024; revised 1 August 2024; accepted 29 August 2024; published 10 September 2024)

Based on our previous work about Coulomb corrections in the trap method [H. Zhang *et al.* *Phys. Lett. B* **850**, 138490 (2024)], we extend the Coulomb-corrected Busch-Englert-Rzażewski-Wilkens formula in coupled-channels nuclear reactions and examine the reliability by taking ${}^4\text{He} = [{}^3\text{H} + p] + [{}^3\text{He} + n]$ as an example. The obtained numerical results are generally well consistent with conventional methods. Our work lays some groundwork for analyzing the coupled-channel reactions involving light charged particles within the trap method.

DOI: [10.1103/PhysRevC.110.034308](https://doi.org/10.1103/PhysRevC.110.034308)

I. INTRODUCTION

As an approach converting scattering between particles into bound-state solutions, the trap method has been successfully applied in lattice quantum chromodynamics (LQCD), atomic physics and nuclear physics. With added artificial traps, the properties of the scattering between two particles in free space can be associated with the discrete positive energy spectrum of the confined system through a closed-form formula, such as the Lüscher formula [1] in periodic cubic box, Busch-Englert-Rzażewski-Wilkens (BERW) formula [2] in harmonic oscillator trap [3–10], and so on. These formulas have also been extended to coupled-channels and few-body sectors [11–17]. Generally speaking, for a two-body system confined in an artificial trap, the formula about scattering phase shift have a form of:

$$\det[\cot(\delta(E)) - \mathcal{F}^{\text{trap}}(E)] = 0, \quad (1)$$

where $\delta(E)$ represents the scattering phase shifts, and the analytic matrix function $\mathcal{F}^{\text{trap}}(E)$ is determined through the geometric and dynamic properties of the trap itself.

In the absence of Coulomb potential, the analytic function $\mathcal{F}^{\text{trap}}(E)$ for harmonic oscillator trap is the so-called Busch-Englert-Rzażewski-Wilkens (BERW) formula:

$$\cot(\delta_l(E)) = (-1)^{l+1} \left(\frac{4\mu\omega}{k^2} \right)^{l+1/2} \frac{\Gamma\left(\frac{3}{4} + \frac{l}{2} - \frac{E}{2\omega}\right)}{\Gamma\left(\frac{1}{4} - \frac{l}{2} - \frac{E}{2\omega}\right)}, \quad (2)$$

where μ is the reduced mass and δ_l is the scattering phase shift. This formula holds at the eigenenergies $E = \frac{k^2}{2\mu}$ with the center-of-mass energy already subtracted.

However, dealing with the long-range Coulomb interaction within various traps has consistently been a significant challenge. It is known that only in some simple situations, such

as the spherical hard walls, the Coulomb potential can be analytically incorporated. For more general cases, the Coulomb corrections are complicated to address. Indeed, some works have already discussed how to handle the Coulomb potential and incorporate the Coulomb corrections in the conventional trap methods [18–25]. In these investigations, the Coulomb-corrected BERW formula [24,25] for harmonic oscillator traps can efficiently treat the Coulomb corrections based on the perturbation expansion.

In our previous work [25] we calculate the proton-proton *s*-wave scattering phase shifts using the Coulomb-corrected BERW formula and validate the reliability of the perturbation expansion approach. Based on these results, in this work we extend the application of the Coulomb-corrected BERW formula to coupled-channels reactions, and calculate the phase shifts and inelasticity of ${}^4\text{He} = [{}^3\text{H} + p] + [{}^3\text{He} + n]$ two-channel cluster model as an example. Additionally, we introduce harmonic oscillator traps with different size in each channel, with such extension of the parameter space the algorithm of the coupled-channels trap method is improved. The results obtained confirm the validity and reliability of Coulomb-corrected BERW formula in solving coupled-channels problems.

The remaining parts are organized as follows. In Sec. II, the Coulomb corrections in harmonic oscillator trap are formulated by the perturbation expansion. With ${}^4\text{He} = [{}^3\text{H} + p] + [{}^3\text{He} + n]$ cluster model as a specific example, we extend the Coulomb-corrected BERW formula to a general two-channel reaction. In Sec. III, the numerical results of ${}^4\text{He} = [{}^3\text{H} + p] + [{}^3\text{He} + n]$ cluster model are presented and discussed. Section IV summarizes the paper. Some derivation about Coulomb-corrected BERW formula in coupled channels are provided in the Appendix.

II. THEORETICAL FORMALISM

A. Coulomb-corrected BERW formula

For the general case involving the Coulomb interaction, the analytic matrix function $\mathcal{F}^{\text{trap}}(E)$ in Eq. (1) can be formulated

*Contact author: zhang_hantao@foxmail.com

†Contact author: dbai@hhu.edu.cn

‡Contact author: zren@tongji.edu.cn

as the following general form [13]:

$$\mathcal{F}_l^{\text{trap}}(E) = \frac{1}{2\mu k^{2l+1} C_L^2(\eta)} \times \left(\Re \left[\frac{G_l^C(r, r', k)}{(rr')^l} \right] \Big|_{r, r' \rightarrow 0} - \frac{G_l^{C, \text{trap}}(r, r', E)}{(rr')^l} \Big|_{r, r' \rightarrow 0} \right), \quad (3)$$

where $C_L(\eta) = 2^L \frac{|\Gamma(L+1+i\eta)|}{(2L+1)!} e^{-\frac{\pi}{2}\eta}$ is the Sommerfeld factor, $G_l^C(r, r', k)$ is the Coulomb Green's function, $G_l^{C, \text{trap}}(r, r', E)$ is the Coulomb force modified Green's function in a trap. Both $G_l^C(r, r', k)$ and $G_l^{C, \text{trap}}(r, r', E)$ are ultraviolet divergent, however, after cancellation between two terms a finite and well-defined function can be obtained.

The Coulomb Green's function in a trap $G^{C, \text{trap}}$ satisfies the Dyson equation:

$$G_l^{C, \text{trap}}(r, r', E) = G_l^{\text{trap}}(r, r', E) + \int_0^\infty dr'' r''^2 G_l^{\text{trap}}(r, r'', E) \times V_C(r'') G_l^{C, \text{trap}}(r'', r', E), \quad (4)$$

where $V_C(r) = \frac{Z_1 Z_2 e^2}{r}$ is the Coulomb potential.

For harmonic oscillator potential $\frac{1}{2}\mu\omega^2 r^2$, trap Green's function $G_l^{\text{trap}}(r, r', E)$ can be written as $G_l^\omega(r, r', E)$ [26]:

$$G_l^\omega(r, r', E) = -\frac{1}{\omega (rr')^{3/2}} \frac{\Gamma(\frac{l}{2} + \frac{3}{4} - \frac{E}{2\omega})}{\Gamma(l + \frac{3}{2})} \times \mathcal{M}_{\frac{E}{2\omega}, \frac{l}{2} + \frac{1}{4}}(\mu\omega r_-^2) \mathcal{W}_{\frac{E}{2\omega}, \frac{l}{2} + \frac{1}{4}}(\mu\omega r_+^2), \quad (5)$$

where $\mathcal{M}_{a,b}(z)$ and $\mathcal{W}_{a,b}(z)$ are the Whittaker functions [27], r_- and r_+ denote the lesser and greater of (r, r') , respectively.

In order to make sure the divergences canceled out properly order by order, $G_l^C(r, r', E)$ is also expanded through the following Dyson equation:

$$G_l^C(r, r', k) = G_l^{\text{free}}(r, r', k) + \int_0^\infty dr'' r''^2 G_l^{\text{free}}(r, r'', k) \times V_C(r'') G_l^C(r'', r', k) \\ G_l^{\text{free}}(r, r', k) = -2i\mu k j_l(kr_-) h_l^{(+)}(kr_+), \quad (6)$$

where j_l and $h_l^{(+)}$ are regular spherical Bessel and Hankel functions. r_- and r_+ denote the lesser and greater of (r, r') , respectively.

According to the Dyson equations above, the perturbation expansion of the Green's functions $G_l^C(r, r', k)$ and $G_l^{C, \text{trap}}(r, r', E)$ can be expressed by operator form as:

$$\hat{G}^C = \frac{\hat{G}^{\text{free}}}{1 - \hat{V}_C \hat{G}^{\text{free}}} = \sum_{n=0}^{\infty} \hat{G}^{\text{free}} (\hat{V}_C \hat{G}^{\text{free}})^n, \\ \hat{G}^{C, \text{trap}} = \frac{\hat{G}^{\text{trap}}}{1 - \hat{V}_C \hat{G}^{\text{trap}}} = \sum_{n=0}^{\infty} \hat{G}^{\text{trap}} (\hat{V}_C \hat{G}^{\text{trap}})^n, \quad (7)$$

where $\hat{G}^{\text{free}} = \frac{1}{E - \hat{H}_0}$, $\hat{G}^{\text{trap}} = \frac{1}{E - \hat{H}_{\text{trap}}}$ and $\hat{H}_0 = -\frac{\hbar^2}{2\mu} \nabla^2$, $\hat{H}_{\text{trap}} = \hat{H}_0 + \frac{1}{2}\mu\omega^2 r^2$.

Therefore, for harmonic oscillator trap, the leading-order (zeroth-order) and n -order perturbation results for $\mathcal{F}^{\text{trap}}(E)$

can be expressed formally as:

$$\mathcal{F}^{\text{trap}, 0\text{th}}(E) = \frac{C_l^2(0)}{C_l^2(\eta)} (-1)^{l+1} \left(\frac{4\mu\omega}{k^2} \right)^{l+1/2} \frac{\Gamma(\frac{3}{4} + \frac{l}{2} - \frac{E}{2\omega})}{\Gamma(\frac{1}{4} - \frac{l}{2} - \frac{E}{2\omega})}, \\ \mathcal{F}^{\text{trap}, n\text{th}}(E) = \frac{1}{2\mu k^{2l+1} C_l^2(\eta)} \frac{\Delta G_l^{n\text{-th}}(r, r', E)}{(rr')^l} \Big|_{r, r' \rightarrow 0}, \quad (8)$$

where corrections $\Delta G_l^{n\text{th}}$ can be obtained with n -dimensional integral according to Eq. (7).

It is noteworthy that there exists a divergent behavior at some particular points $\frac{E}{\omega} = \frac{3}{2} + l + 2N$, $N = 0, 1, 2, \dots$, which correspond to the eigenenergies of noninteracting particles in the harmonic trap. When nearing these anomalous points, the convergence of Coulomb-corrected BERW formula will become slow or even fail [25]. Indeed, this kind of divergence is a common problem within the trap method. If we define the eigenenergies of noninteracting particles in the trap as the trap's eigenenergies, the trap method will completely fail when the eigenenergies of the trapped system coincide with the trap's eigenenergies.

In practice, on account of the internal structure of the particles, the effective Coulomb potential is usually written in a form of the error function:

$$V_C^{\text{eff}} = \frac{Z_1 Z_2 e^2}{r} \text{erf}(\sqrt{\beta}r), \quad (9)$$

where $\beta > 0$ is a parameter determined by reproduce some important properties of the considered system, such as the charge radius and so on. In order to apply the above procedure of the Coulomb corrections in such cases, the effective Coulomb interaction can be rewritten as:

$$V_C^{\text{eff}} = \frac{Z_1 Z_2 e^2}{r} [\text{erf}(\sqrt{\beta}r) - 1] + \frac{Z_1 Z_2 e^2}{r}, \quad (10)$$

the first term becomes a short-range interaction, which can be included in the original short-range interactions. Similarly, for other forms of effective Coulomb potential V_C^{eff} , once it can quickly converge to V_C , the Coulomb corrections can be achieved as the same as the case of bare Coulomb potential.

The application of the trap method requires interaction-independent modeling. For a harmonic oscillator trap, the frequency ω should be restricted to be small (further details can be found in the Appendix), therefore large size of the harmonic trap requires much more basis functions to reproduce the correct long-range behavior of the wave functions. Moreover, each additional order in the perturbation expansion increases the dimension of the integrals by one. In order to obtain convergent phase shifts, it often requires expanding to a high number of orders, sometimes up to the tenth order or even higher, especially in regions where convergence is slow (close to the divergent points). This significantly raises the computational time because of the high-dimensional integrals. Even with Monte Carlo integration methods, the numerical burden is already quite evident in two-body problems. These disadvantages will significantly limit the application of coupled-channels Coulomb-corrected BERW formula in *ab initio* calculations.

B. Coupled-channel system in traps

For a general coupled-channels (two-channels) system, the Schrödinger equation can be written as:

$$\begin{aligned} \left[-\frac{\hbar^2}{2\mu_1} \nabla^2 + V_{11}(r) + E_1 \right] \phi_1(r) + V_{12} \phi_2(r) &= E \phi_1(r), \\ \left[-\frac{\hbar^2}{2\mu_2} \nabla^2 + V_{22}(r) + E_2 \right] \phi_2(r) + V_{21} \phi_1(r) &= E \phi_2(r), \end{aligned} \quad (11)$$

where E_1 and E_2 represent the threshold energies of two channels, respectively.

$$\begin{aligned} V_{11}(r) &= \text{erf}(\sqrt{\beta}r) \frac{e^2}{r} + \frac{1}{2} \left\{ V_{T=1} \exp \left[-\left(\frac{r}{b_{T=1}} \right)^2 \right] + V_{T=0} \exp \left[-\left(\frac{r}{b_{T=0}} \right)^2 \right] \right\}, \\ V_{22}(r) &= \frac{1}{2} \left\{ V_{T=1} \exp \left[-\left(\frac{r}{b_{T=1}} \right)^2 \right] + V_{T=0} \exp \left[-\left(\frac{r}{b_{T=0}} \right)^2 \right] \right\}, \\ V_{12}(r) &= V_{21}(r) \\ &= \frac{1}{2} \left\{ V_{T=1} \exp \left[-\left(\frac{r}{b_{T=1}} \right)^2 \right] - V_{T=0} \exp \left[-\left(\frac{r}{b_{T=0}} \right)^2 \right] \right\}, \end{aligned} \quad (13)$$

where β is taken to be 0.66 fm^{-2} from the observed r.m.s. radius of ${}^3\text{H}$. In the following calculations, we take 3P_1 state as an example. The parameters in the potential can be found in Refs. [28,29]. The reduced masses are taken as $\mu_1 = \mu_2 = \frac{3}{4}m_N$, where $m_N = 938.918 \text{ MeV}$ is the nucleon mass.

2. Coupled-channel Coulomb-corrected BERW formula

In the case of a two-channel problem, the diagonal harmonic oscillator potential is

$$V_{\text{H.O.}}(r, \omega_1, \omega_2) = \begin{pmatrix} \frac{1}{2}\mu_1\omega_1^2 r^2 & 0 \\ 0 & \frac{1}{2}\mu_2\omega_2^2 r^2 \end{pmatrix}, \quad (14)$$

what should be noted here is that parameters ω_1 and ω_2 can be distinct. Similarly, for more general multichannel systems, the parameters ω in the harmonic oscillator traps for each channel can also be different. Furthermore, for other forms of traps, the parameters in traps in each channel can also be taken with different values. For instance, in a spherical hard wall trap, one can consider various radii, while in a periodic cubic box, different side lengths can be considered. By introducing the different ω the parameter space of the harmonic traps is expanded, based on which the computational approach can be improved. We will make a detailed discussion about this in the subsequent sections.

Similar to the single-channel case, the Coulomb-corrected BERW formula for coupled channels can also be derived through the corresponding quantization condition. Here, we provide the compact form of the determinant condition, and the detailed derivation can be found in the Appendix or

In the following, we apply the coupled-channels Coulomb-corrected BERW formula to coupled-cluster system ${}^4\text{He} = [{}^3\text{H} + p] + [{}^3\text{He} + n]$ as an example.

I. ${}^4\text{He} = [{}^3\text{H} + p] + [{}^3\text{He} + n]$

We denote the ${}^3\text{H} + p$ channel as channel 1, and the ${}^3\text{He} + n$ channel as channel 2. The experimental threshold energy difference between ${}^3\text{He} + n$ and ${}^3\text{H} + p$ channels is used as:

$$E_2 - E_1 = 0.763 \text{ MeV}, \quad (12)$$

where threshold E_1 is set to be the zero point of the energy.

The diagonal potential and the coupling potential are constructed from $T = 1$ and $T = 0$ components:

Ref. [30].

$$\begin{aligned} \mathcal{B}(\delta_{l_1}(E), \delta_{l_2}(E), \eta(E), \omega_1, \omega_2) &= \eta(1 + \mathcal{F}_{l_1}^{\omega_1} \mathcal{F}_{l_2}^{\omega_2}) \cos(\delta_{l_1} - \delta_{l_2}) \\ &+ (1 - \mathcal{F}_{l_1}^{\omega_1} \mathcal{F}_{l_2}^{\omega_2}) \cos(\delta_{l_1} + \delta_{l_2}) \\ &- \eta(\mathcal{F}_{l_1}^{\omega_1} - \mathcal{F}_{l_2}^{\omega_2}) \sin(\delta_{l_1} - \delta_{l_2}) \\ &- (\mathcal{F}_{l_1}^{\omega_1} + \mathcal{F}_{l_2}^{\omega_2}) \sin(\delta_{l_1} + \delta_{l_2}) \\ &= 0, \end{aligned} \quad (15)$$

where \mathcal{F}_i^ω ($i = 1, 2$) represent the analytic matrix functions of two channels with angular momentum l_i ($i = 1, 2$), respectively. $\delta_i(E)$ ($i = 1, 2$) are two scattering phase shifts with E being center-of-mass energy. η is the inelasticity introduced by the parametrization of coupled-channels scattering matrix S :

$$S = \begin{pmatrix} \eta e^{2i\delta_1} & i\sqrt{1-\eta^2} e^{i(\delta_1+\delta_2)} \\ i\sqrt{1-\eta^2} e^{i(\delta_1+\delta_2)} & \eta e^{2i\delta_2} \end{pmatrix}. \quad (16)$$

For the three unknowns: phase shifts δ_1 and δ_2 , and inelasticity η , only Eq. (15) imposes a constraint. Hence, to determine these three quantities, multiple energy-degenerate states are required, each corresponding to different parameters (ω_1, ω_2) . For example, one can solve nonlinear equations using three energy-degenerate states, or more generally, one can select more than three energy-degenerate states to minimize $\sum_{(\omega_1, \omega_2)} \mathcal{B}^2(\delta_1(E), \delta_2(E), \eta(E), \omega_1, \omega_2)$.

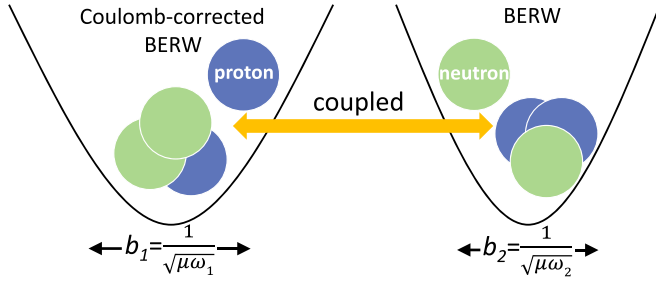


FIG. 1. Illustration for ${}^4\text{He} = [{}^3\text{H} + p] + [{}^3\text{He} + n]$ cluster model in harmonic traps. On the left is the ${}^3\text{H} + p$ system (channel 1) in a harmonic trap, while on the right is the ${}^3\text{He} + n$ system (channel 2) in another harmonic trap. Since only channel 1 involves Coulomb interactions, we utilize the Coulomb-corrected BERW formula for channel 1 and the BERW formula for channel 2. As illustrated, the ω parameters for the harmonic traps can be different in different channels.

III. NUMERICAL RESULTS

We use ${}^4\text{He}$ system (illustrated in Fig. 1) as an example to discuss the application of the Coulomb-corrected BERW formula in coupled-channels calculations. In this case, we only need to consider the Coulomb corrections in ${}^3\text{H} + p$ channel (channel 1). When the total energy exceeds the threshold energy of channel 2 at 0.763 MeV, Eq. (15) is employed to compute the scattering phase shifts and inelasticity, while below the threshold channel 2 is closed and thus δ_2 and inelasticity all vanish, the phase shift for channel 1 can be obtained by the single-channel Coulomb-corrected BERW formula [Eq. (8)].

First, we employ the coupled-channels trap method in the absence of Coulomb potential and different parameters $\omega_1 \neq \omega_2$ are utilized in determining degenerate states. The obtained scattering phase shifts and inelasticity are displayed in Fig. 2. The solid lines represent the results obtained using the coupled-channels R -matrix method [31], while solid square, circle, and triangle markers correspond to δ_1 , δ_2 , and η obtained through Eq. (15). Hollow square markers below the threshold represent results obtained using Eq. (2). The results obtained from the coupled-channels trap method show good agreement with those from the R -matrix method, which provides initial validation of the reliability and accuracy of calculations with different ω parameters. Next, we will focus on discussing the case with Coulomb potential, and highlight the necessity of using different ω parameters in this situation.

First, if considering the case where $\omega_1 = \omega_2$, we can obtain the energy spectrum in the presence of Coulomb potential as shown in Fig. 3. The results for the first eight eigenstates from solving the coupled-channels Schrödinger equation are displayed, with ω ranging from 0.25–1. The horizontal axis represents the eigenenergy E , and the vertical axis represents the ratio of eigenenergy E to ω . We have also indicated the positions of divergent points by horizontal shaded regions, which denote the range of ± 0.05 around divergent points 2.5, 4.5, 6.5, 8.5, 10.5. Following the previously mentioned minimization of $\sum_{(\omega_1, \omega_2)} \mathcal{B}^2(\delta_1(E), \delta_2(E), \eta(E), \omega_1, \omega_2)$, at least three degenerate states are required for a specific

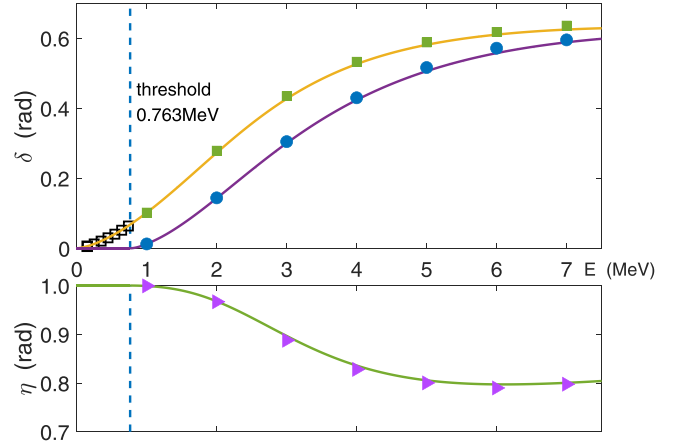


FIG. 2. In the absence of Coulomb potential, the calculated scattering phase shifts and inelasticity of the 3P_1 state. The solid square, circle, and triangle markers represent the phase shifts for channel 1 and channel 2 and inelasticity obtained through the coupled-channels trap method, respectively. The solid lines correspond to the results obtained using the coupled-channels R -matrix method. The threshold energy $E_2 - E_1 = 0.763$ MeV is marked with dashed line. To distinguish between the coupled trap method and the single-channel trap method, hollow square markers are used for the phase shifts of channel 1 below the threshold.

scattering energy E . However, due to the presence of divergence in the Coulomb-corrected BERW formula at certain singular points, the convergence might become notably slow for states near the divergent points. Therefore, such method of selecting degenerate states has some limitations. For example, the vertical dashed line in Fig. 3 corresponds to scattering energy $E = 3$ MeV, we can observe that apart from the

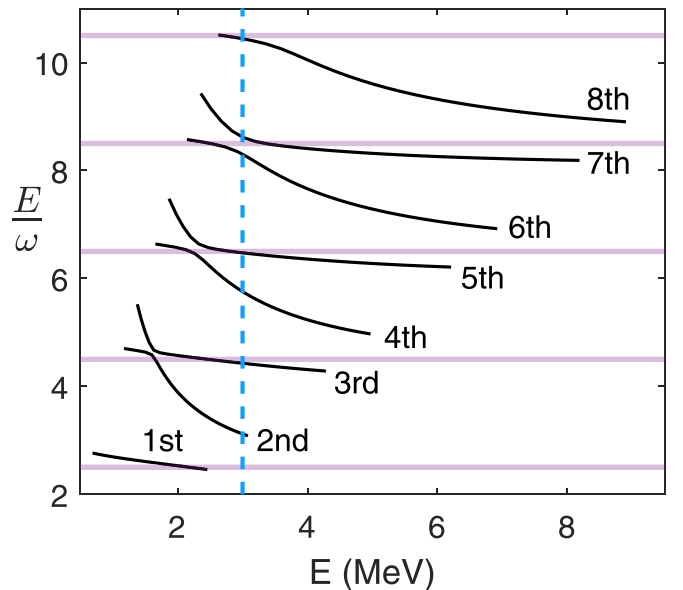


FIG. 3. Plot of the ratio $\frac{E}{\omega}$ as a function of the eigenenergy E . Solid lines represent the results for the first eight eigenstates. Horizontal shaded regions denote the range of ± 0.05 around divergent points 2.5, 4.5, 6.5, 8.5, 10.5.

intersections with the curves of the second and fourth eigenenergies, the other intersections are quite close to the divergent points. Such limitations will lead to extensive computational time when using Coulomb-corrected BERW formula, or even cause the failure of convergence.

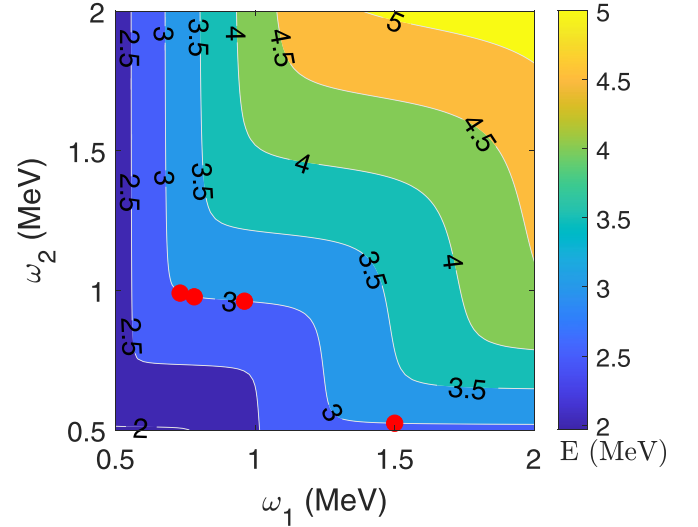
In order to avoid such problems, expanding the parameter space of the harmonic traps is necessary and effective. When we introduce different ω in two channels, we can obtain the energy surface and contour plots for ratio $\frac{E}{\omega_1}$ presented in Fig. 4 (for the second eigenstate), where the positions of divergent points are marked with red lines. With the help of the extra degree of freedom by an added ω , the possibilities for selecting degenerate states after avoiding the divergent points are significantly increased. Undoubtedly, this approach allows for better achievement of the minimization goal for $\sum_{(\omega_1, \omega_2)} \mathcal{B}^2(\delta_1(E), \delta_2(E), \eta(E), \omega_1, \omega_2)$, while effectively reducing the computational load of Coulomb corrections.

Here, we take the energy point $E = 3$ MeV as an example to demonstrate the usage of our method. At first, we select four degenerate states (belonging to the second eigenstate) as shown in Fig. 3. In the selection, the points are chosen away from red lines as much as possible to avoid divergent points in Coulomb correction, of course, ω should not be too large. Next, by minimizing $\sum_{(\omega_1, \omega_2)} \mathcal{B}^2(\delta_1(E), \delta_2(E), \eta(E), \omega_1, \omega_2)$ we can obtain the unknowns δ_1 , δ_2 , and η . Additionally, to display the convergence of the Coulomb corrections, we present the scattering phase shifts and inelasticity at different Coulomb correction orders in Fig. 5. It is evident that as the correction order increases, δ_1 , δ_2 , and η tend to stabilize. In our actual calculations for the $E = 3$ MeV energy point, we choose results with the sixth-order correction. For other scattering energies, our calculation approach remains similar. It is noteworthy that in the calculation for $E = 3$ MeV, four degenerate states are all belong to the second eigenstate. However, the degenerate states from the eigenstates with different indices can also be incorporated.

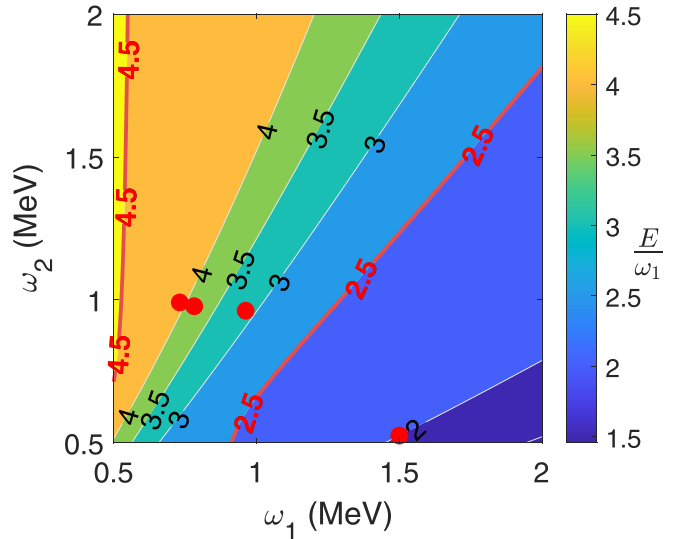
Figure 6 displays the phase shifts and inelasticity obtained using the coupled-channels Coulomb-corrected BERW formula for the 3P_1 state of ${}^4\text{He}$ system. The solid square and circular markers represent the phase shifts of channel 1 and channel 2, respectively, while the solid triangle markers represent the inelasticity. The solid lines correspond to the results obtained by coupled channel R -matrix method. It is evident that the calculations using the Coulomb-corrected BERW formula in coupled channels are in good agreement with the traditional method.

IV. CONCLUSIONS

As an extension of the application of the Coulomb-corrected BERW formula, we employ it to investigate the coupled-channels reactions involving light charged particles. By taking ${}^4\text{He} = [{}^3\text{H} + p] + [{}^3\text{He} + n]$ system as an example, we compute the corresponding scattering phase shifts and inelasticity. Additionally, we employ different ω parameters in harmonic oscillator potentials for each channel, which allows us to expand the parameter space to avoid the anomalous



(a) Energy contour in the parameter space (ω_1, ω_2)



(b) Contour of the ratio $\frac{E}{\omega_1}$ in the parameter space (ω_1, ω_2)

FIG. 4. (a) The energy contour of the second eigenstate in the parameter space (ω_1, ω_2) . (b) The ratio $\frac{E}{\omega_1}$ in the parameter space (ω_1, ω_2) . As channel 1 contains the Coulomb potential, we only plotted the contour map for $\frac{E}{\omega_1}$. For channel 2, any point (ω_1, ω_2) not located the divergence points is acceptable. Here, we marked the ω parameters corresponding to divergence points with red lines. Avoiding these parameter points in calculations can contribute to a faster convergence of Coulomb corrections. The four states with degenerate energy $E = 3$ MeV used in the calculations are marked with red dots in the figure.

points and reduce the calculation amount in the Coulomb correction computations. The numerical results obtained by our method provide good validation of the reliability of Coulomb-corrected BERW formula in coupled-channels calculations. This work lays some groundwork in studying the coupled-channels problems involving light charged clusters within the trap method. The application of our approach in *ab initio* computations is limited by shortcomings of small ω

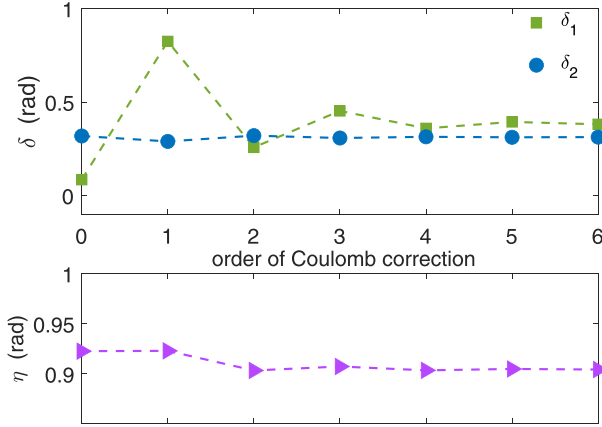


FIG. 5. Top panel: Phase shifts for different orders of Coulomb correction with $E = 3$ MeV. Circle and square markers correspond to the phase shifts for channel 1 and channel 2, respectively. Bottom panel: Inelasticity for different orders of Coulomb correction with $E = 3$ MeV.

and complicated perturbation expansion. In the future we will investigate how to overcome these disadvantages and attempt to handle both neutral and charged particle scattering within *ab initio* frameworks.

ACKNOWLEDGMENTS

This work is supported by the National Natural Science Foundation of China (Grants No. 12035011, No. 11905103, No. 11947211, No. 11761161001, No. 11961141003, No. 12022517 and No. 12375122), by the National Key R&D Program of China (Contract No. 2023YFA1606503), by the Science and Technology Development Fund of Macau (Grants No. 0048/2020/A1 and No. 008/2017/AFJ), by the Funda-

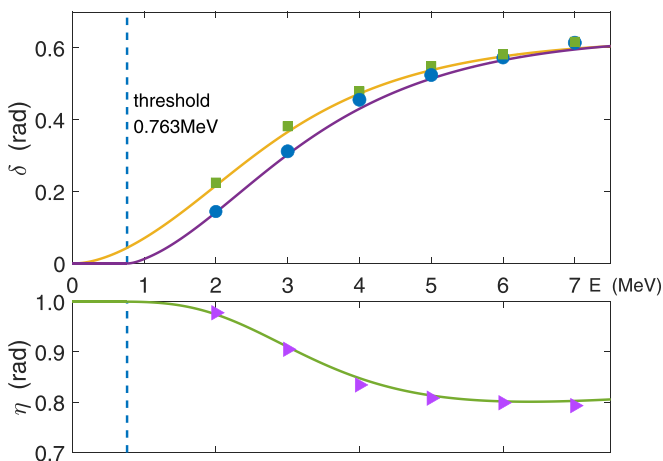


FIG. 6. In the presence of Coulomb potential, the calculated scattering phase shifts and inelasticity of the 3P_1 state. The solid square, circle, and triangle markers represent the phase shifts for channel 1 and channel 2 and inelasticity obtained through the coupled-channels trap method, respectively. The solid lines correspond to the results obtained using the coupled-channels R -matrix method. The threshold energy $E_2 - E_1 = 0.763$ MeV is marked with dashed line.

mental Research Funds for the Central Universities (Grants No. 22120210138 and No. 22120200101).

APPENDIX: QUANTIZATION CONDITION IN COUPLED-CHANNEL REACTION

For single-channel two-body system in the presence of Coulomb potential, the original Hamiltonian H and the Hamiltonian of the trapped system H^* can be written as

$$\hat{H} = -\frac{\hbar^2}{2\mu}\nabla^2 + \hat{V} + \hat{V}_C = \hat{H}_0 + \hat{V} + \hat{V}_C,$$

$$\hat{H}^* = \hat{H}_0 + \hat{V} + \hat{V}_C + \hat{U} = \hat{H}_{\text{trap}} + \hat{V} + \hat{V}_C, \quad (\text{A1})$$

where V is the short-range interaction, V_C is the Coulomb interaction, and U is the artificial potential well. The scattering properties in infinite space can be expressed with the Lippmann-Schwinger equation,

$$\hat{T}(E) = -\hat{V} + \hat{V}\hat{G}^C(E)\hat{T}(E), \quad (\text{A2})$$

where \hat{T} is the T matrix, E is the center-of-mass energy and $\hat{G}^C(E) = \frac{1}{E - (\hat{H}_0 + \hat{V}_C)}$ is the Green's function within the Coulomb potential. T matrix can be solved formally from the Lippmann-Schwinger equation,

$$\hat{T}(E) = -[\hat{V}^{-1} - \hat{G}^C(E)]^{-1}. \quad (\text{A3})$$

In order to perform an interaction-independent modeling, the range b_V of the short-range interaction V should be much smaller than the spatial size b_U of the artificial potential well U . In other words, we can find a region within the potential well where the short-range interaction can be neglected. In this case, a connection between the asymptotic form of the scattering wave function with the wave function of bound state can be constructed. For the harmonic oscillator trap, two spatial scales need to satisfy $b_V \ll b_\omega = \frac{\hbar}{\sqrt{\mu\omega}}$, namely the frequency ω should be as small as possible.

With the artificial potential well U , which satisfies the above interaction-independent modeling, we can define another T_{trap} matrix for the trapped system,

$$\hat{T}_{\text{trap}}(E) = -\hat{V} + \hat{V}\hat{G}^{C,\text{trap}}(E)\hat{T}_{\text{trap}}(E), \quad (\text{A4})$$

where $\hat{G}^{C,\text{trap}} = \frac{1}{E - (\hat{H}_0 + \hat{V}_C + \hat{U})}$ is the Green's function within the Coulomb potential and the artificial potential U .

Similarly, T matrix in the trap can also be solved formally,

$$\hat{T}_{\text{trap}}(E) = -[\hat{V}^{-1} - \hat{G}^{C,\text{trap}}(E)]^{-1}, \quad (\text{A5})$$

and the bound states with energy E_b in the trap are determined by the poles of $\hat{T}_{\text{trap}}(E)$, therefore we can obtain a determinant condition for any E_b ,

$$\det[\hat{V}^{-1} - \hat{G}^{C,\text{trap}}(E_b)] = 0. \quad (\text{A6})$$

Therefore, by considering both Eqs. (A3) and (A6) one can obtain the quantization condition in determinant form as,

$$\det[\hat{T}^{-1}(E_b) + \hat{G}^{C,\text{trap}}(E_b) - \hat{G}^C(E_b)] = 0. \quad (\text{A7})$$

In the following we provide a concise derivation of Eq. (15). Here, we consider a two-channel reaction, each channel composed of two distinguishable particles. Namely,

we can represent this reaction as: $A + B \rightarrow C + D$. We label the left-hand side as channel 1 and the right-hand side as channel 2. The orbital angular momenta of the two channels are denoted as l_1 and l_2 . The quantization condition of two-channel two-body system has the same determinant form as Eq. (A7) in the single-channel case. The difference is that \hat{T} , $\hat{G}^{C,\text{trap}}$, and \hat{G}^C all become 2×2 matrices in two-channel reactions.

In addition, with the introduction of the separable form of the potential [30], T matrix can be written as

$T_l(k, k') = (kk')^l t_l(E)$, and therefore when it is on-shell, the Coulomb modified scattering amplitude matrix t_l is usually parameterized by phase shifts, δ_{l_1} , δ_{l_2} and inelasticity η as:

$$\frac{t(E)}{(4\pi)^2} = \begin{pmatrix} \frac{-i(\eta e^{2i\delta_{l_1}} - 1)}{4\mu_1 k_1^{2l_1+1}} & \frac{\sqrt{1-\eta^2} e^{i(\delta_{l_1} + \delta_{l_2})}}{4\mu_1 k_1^{l_1} k_2^{l_2}} \\ \frac{\sqrt{1-\eta^2} e^{i(\delta_{l_1} + \delta_{l_2})}}{4\mu_2 k_2^{l_2} k_1^{l_1}} & \frac{-i(\eta e^{2i\delta_{l_2}} - 1)}{4\mu_2 k_2^{2l_2+1}} \end{pmatrix}. \quad (\text{A8})$$

Through quantization conditions, we can obtain the determinant condition in coordinate space as:

$$\det \left[\frac{1}{C_l^2(\eta)} \frac{G_l^{C,\text{trap}}(r, r', E) - G_l^C(r, r', k)}{(rr')^l} \Big|_{r, r' \rightarrow 0} + (4\pi)^2 t^{-1}(E) \right] = 0. \quad (\text{A9})$$

For the first term in determinant, we use l to denote the angular momentum. In fact, this term can be written as 2×2 matrix:

$$\begin{pmatrix} \frac{1}{C_{l_1}^2(\eta)} \frac{G_{l_1}^{C,\text{trap}}(r, r', E) - G_{l_1}^C(r, r', k)}{(rr')^{l_1}} \Big|_{r, r' \rightarrow 0} & 0 \\ 0 & \frac{1}{C_{l_2}^2(\eta)} \frac{G_{l_2}^{C,\text{trap}}(r, r', E) - G_{l_2}^C(r, r', k)}{(rr')^{l_2}} \Big|_{r, r' \rightarrow 0} \end{pmatrix}. \quad (\text{A10})$$

Here, we present the general form that includes the Coulomb potential. It is noteworthy that Eq. (A9) remains valid even if some channels do not include the Coulomb potential. Clearly, when the Coulomb potentials are absence in some channels, the corresponding diagonal elements in (A10) naturally reduces to the case of BERW formula. It is also worth noting that the procedure is similar for multichannel cases.

We have already known that

$$\frac{1}{C_l^2(\eta)} \Im [G_l^C(r, r', k)] \Big|_{r, r' \rightarrow 0} = -2\mu k^{2l+1},$$

$$\mathcal{F}_l^{\text{trap}}(E) = \frac{1}{2\mu k^{2l+1} C_l^2(\eta)} \left(\Re [G_l^C(r, r', k)] \Big|_{r, r' \rightarrow 0} - \frac{G_l^{C,\text{trap}}(r, r', E)}{(rr')^l} \Big|_{r, r' \rightarrow 0} \right). \quad (\text{A11})$$

Therefore, the determinant condition (A9) becomes:

$$\det \left[C_{1,2} \begin{pmatrix} -i(\eta e^{2i\delta_{l_2}} - 1)\mu_1 k_1^{2l_1+1} & -\sqrt{1-\eta^2} e^{i(\delta_{l_1} + \delta_{l_2})} \mu_2 k_2^{l_2+1} k_1^{l_1} \\ -\sqrt{1-\eta^2} e^{i(\delta_{l_1} + \delta_{l_2})} \mu_1 k_1^{l_1+1} k_2^{l_2} & -i(\eta e^{2i\delta_{l_1}} - 1)\mu_2 k_2^{2l_2+1} \end{pmatrix} + \begin{pmatrix} 2\mu_1 k_1^{2l_1+1} (-\mathcal{F}_{l_1} + i) & 0 \\ 0 & 2\mu_2 k_2^{2l_2+1} (-\mathcal{F}_{l_2} + i) \end{pmatrix} \right] = 0, \quad (\text{A12})$$

where $C_{1,2} = \frac{4}{\eta(e^{2i\delta_{l_1}} + e^{2i\delta_{l_2}}) - e^{2i(\delta_{l_1} + \delta_{l_2})} - 1}$.

After computation we can obtain:

$$\frac{-\eta(1 + \mathcal{F}_1 \mathcal{F}_2) \cos(\delta_1 - \delta_2) + (-1 + \mathcal{F}_1 \mathcal{F}_2) \cos(\delta_1 + \delta_2) + \eta(\mathcal{F}_1 - \mathcal{F}_2) \sin(\delta_1 - \delta_2) + (\mathcal{F}_1 + \mathcal{F}_2) \sin(\delta_1 + \delta_2)}{-\eta \cos(\delta_1 - \delta_2) + \cos(\delta_1 + \delta_2)} = 0. \quad (\text{A13})$$

Namely the formula in Eq. (15):

$$-\eta(1 + \mathcal{F}_1 \mathcal{F}_2) \cos(\delta_1 - \delta_2) + (-1 + \mathcal{F}_1 \mathcal{F}_2) \cos(\delta_1 + \delta_2) + \eta(\mathcal{F}_1 - \mathcal{F}_2) \sin(\delta_1 - \delta_2) + (\mathcal{F}_1 + \mathcal{F}_2) \sin(\delta_1 + \delta_2) = 0. \quad (\text{A14})$$

It is straightforward to verify that when inelasticity η equals 1 (complete elastic), the above equation degenerates into the noncoupled form. Equation (15) provides a clear and unified way to describe coupled-channels systems. Whether or not there is a Coulomb potential, we only need to substitute the \mathcal{F} function corresponding to each channel into Eq. (A14).

[1] M. Lüscher, *Nucl. Phys. B* **354**, 531 (1991).

[2] T. Busch, B.-G. Englert, K. Rzazewski, and M. Wilkens, *Found. Phys.* **28**, 549 (1998).

[3] X. Zhang, *Phys. Rev. C* **101**, 051602(R) (2020).

[4] T. Luu, M. J. Savage, A. Schwenk, and J. P. Vary, *Phys. Rev. C* **82**, 034003 (2010).

- [5] X. Zhang, S. R. Stroberg, P. Navrátil, C. Gwak, J. A. Melendez, R. J. Furnstahl, and J. D. Holt, *Phys. Rev. Lett.* **125**, 112503 (2020).
- [6] I. Stetcu, J. Rotureau, B. Barrett, and U. van Kolck, *Ann. Phys. (NY)* **325**, 1644 (2010).
- [7] M. Bagnarol, M. Schäfer, B. Bazak, and N. Barnea, *Phys. Lett. B* **844**, 138078 (2023).
- [8] M. Schäfer and B. Bazak, *Phys. Rev. C* **107**, 064001 (2023).
- [9] H. Zhang, D. Bai, Z. Wang, and Z. Ren, *Phys. Rev. C* **109**, 034307 (2024).
- [10] H. Zhang, D. Bai, and Z. Ren, *Phys. Lett. B* **855**, 138861 (2024).
- [11] J. Rotureau, I. Stetcu, B. R. Barrett, and U. van Kolck, *Phys. Rev. C* **85**, 034003 (2012).
- [12] P. Guo, *Phys. Lett. B* **804**, 135370 (2020).
- [13] P. Guo and V. Gasparian, *Phys. Rev. D* **103**, 094520 (2021).
- [14] S. He, X. Feng, and C. Liu, *J. High Energy Phys.* **07** (2005) 011.
- [15] P. Guo, J. J. Dudek, R. G. Edwards, and A. P. Szczepaniak, *Phys. Rev. D* **88**, 014501 (2013).
- [16] S. Kreuzer and H.-W. Hammer, *Phys. Lett. B* **673**, 260 (2009).
- [17] M. Mai and M. Döring, *Phys. Rev. Lett.* **122**, 062503 (2019).
- [18] R. Bubna, H.-W. Hammer, F. Müller, J.-Y. Pang, A. Rusetsky, and J.-J. Wu, *J. High Energy Phys.* **05** (2024) 168.
- [19] H. Yu, S. König, and D. Lee, *Phys. Rev. Lett.* **131**, 212502 (2023).
- [20] N. Christ, X. Feng, J. Karpie, and T. Nguyen, *Phys. Rev. D* **106**, 014508 (2022).
- [21] Z. Davoudi, J. Harrison, A. Jüttner, A. Portelli, and M. J. Savage, *Phys. Rev. D* **99**, 034510 (2019).
- [22] U. Stellin and G. Meißner, *Eur. Phys. J. A* **57**, 26 (2021).
- [23] S. R. Beane and M. J. Savage, *Phys. Rev. D* **90**, 074511 (2014).
- [24] P. Guo, *Phys. Rev. C* **103**, 064611 (2021).
- [25] H. Zhang, D. Bai, Z. Wang, and Z. Ren, *Phys. Lett. B* **850**, 138490 (2024).
- [26] S. Blinder, *J. Math. Phys.* **25**, 905 (1984).
- [27] DLMF, *NIST Digital Library of Mathematical Functions*, <https://dlmf.nist.gov/>, Release 1.1.11 of 2023-09-15, 2023, edited by F. W. J. Olver, A. B. Olde Daalhuis, D. W. Lozier, B. I. Schneider, R. F. Boisvert, C. W. Clark, B. R. Miller, B. V. Saunders, H. S. Cohl, and M. A. McClain.
- [28] R. Suzuki, A. T. Kruppa, B. G. Giraud, and K. Kat, *Prog. Theor. Phys.* **119**, 949 (2008).
- [29] M. Odsuren, T. Myo, Y. Kikuchi, M. Teshigawara, and K. Katō, *Phys. Rev. C* **104**, 014325 (2021).
- [30] P. Guo and B. Long, *J. Phys. G: Nucl. Part. Phys.* **49**, 055104 (2022).
- [31] P. Descouvemont and D. Baye, *Rep. Prog. Phys.* **73**, 036301 (2010).